European Radiology (2021) 31:4700–4709
https://doi.org/10.1007/s00330-020-07566-2

GASTROINTESTINAL

Diagnostic value of deep learning reconstruction for radiation dose reduction at abdominal ultra-high-resolution CT

Yuko Nakamura[1] · Keigo Narita[1] · Toru Higaki[1] · Motonori Akagi[1] · Yukiko Honda[1] · Kazuo Awai[1]

Received: 12 July 2020 / Revised: 1 October 2020 / Accepted: 26 November 2020 / Published online: 3 January 2021

Abstract

Objectives We evaluated lower dose (LD) hepatic dynamic ultra-high-resolution computed tomography (U-HRCT) images reconstructed with deep learning reconstruction (DLR), hybrid iterative reconstruction (hybrid-IR), or model-based IR (MBIR) in comparison with standard-dose (SD) U-HRCT images reconstructed with hybrid-IR as the reference standard to identify the method that allowed for the greatest radiation dose reduction while preserving the diagnostic value.

Methods Evaluated were 72 patients who had undergone hepatic dynamic U-HRCT; 36 were scanned with the standard radiation dose (SD group) and 36 with 70% of the SD (lower dose [LD] group). Hepatic arterial and equilibrium phase (HAP, EP) images were reconstructed with hybrid-IR in the SD group, and with hybrid-IR, MBIR, and DLR in the LD group. One radiologist recorded the standard deviation of attenuation in the paraspinal muscle as the image noise. The overall image quality was assessed by 3 other radiologists; they used a 5-point confidence scale ranging from 1 (unacceptable) to 5 (excellent). Superiority and equivalence with prespecified margins were assessed.

Results With respect to the image noise, in the HAP and EP, LD DLR and LD MBIR images were superior to SD hybrid-IR images; LD hybrid-IR images were neither superior nor equivalent to SD hybrid-IR images. With respect to the quality scores, only LD DLR images were superior to SD hybrid-IR images.

Conclusions DLR preserved the quality of abdominal U-HRCT images even when scanned with a reduced radiation dose.

Key Points

- *Lower dose DLR images were superior to the standard-dose hybrid-IR images quantitatively and qualitatively at abdominal U-HRCT.*
- *Neither hybrid-IR nor MBIR may allow for a radiation dose reduction at abdominal U-HRCT without compromising the image quality.*
- *Because DLR allows for a reduction in the radiation dose and maintains the image quality even at the thinnest slice section, DLR should be applied to abdominal U-HRCT scans.*

Keywords Liver · Tomography, X-ray computed · Deep learning · Radiation dosage

Abbreviations

AiCE	Advanced Intelligent Clear-IQ Engine
AIDR3D	Adaptive Iterative Dose Reduction 3-Dimensional
BMI	Body mass index
CA	Chromosomal aberrations
CI	Confidence interval
CNR	Contrast-to-noise ratio
$CTDI_{vol}$	CT dose index
DICOM	Digital Imaging and Communications in Medicine
DLP	Dose-length product
DLR	Deep learning reconstruction
EP	Equilibrium phase
FIRST	Forward projected model based iterative reconstruction solution
HAP	Hepatic arterial phase
Hybrid-IR	Hybrid iterative reconstruction
LD	Lower dose
MBIR	Model-based iterative reconstruction

✉ Yuko Nakamura
yukon@hiroshima-u.ac.jp

[1] Diagnostic Radiology, Hiroshima University, 1-2-3 Kasumi, Minami-ku, Hiroshima 734-8551, Japan

ROI	Region of interest
SD	Standard dose
SSDE	Size-specific dose estimate
U-HRCT	Ultra-high-resolution computed tomography

Introduction

Ultra-high-resolution computed tomography (U-HRCT) involves a smaller detector element and tube focus size than conventional CT. It yields images of higher spatial resolution; their usefulness for the examination of lungs and coronary and peripheral arteries has been reported [1–4]. For abdominal studies, the higher resolution on U-HRCT scans renders it superior to conventional CT for the visualization of smaller bile ducts on drip-infusion CT cholangiograms [5]. However, due to its smaller detectors, higher radiation doses are required especially for abdominal U-HRCT because the noise is higher than on conventional CT scans [1, 4, 6].

Reconstruction methods should yield images with the lowest possible image noise without sacrificing image accuracy and spatial resolution. Model-based iterative reconstruction (MBIR), an advanced reconstruction algorithm for CT studies, can improve the image quality and allow for a radiation-dose reduction [7–9]. However, the improved detectability on MBIR images of low-contrast lesions, particularly at low-dose tube flux levels and in larger patients, remains to be demonstrated [10–12]. Moreover, the MBIR approach tends to require high computational power and longer reconstruction times than hybrid iterative reconstruction (hybrid-IR) which is faster and more widely used although its overall imaging performance is inferior to MBIR in terms of noise and artifact reduction [7, 13–15].

Deep learning reconstruction (DLR, Advanced Intelligent Clear-IQ Engine (AiCE), Canon Medical Systems), the first commercialized deep-learning reconstruction tool, introduces deep convolutional neural networks that are trained on a teaching dataset of ideal MBIR images into the reconstruction flow [16–20]. The image quality of abdominal CT scans has been reported to be better on U-HRCT images subjected to DLR than MBIR [16]. In addition, according to Singh et al [21], when conventional chest and abdominopelvic CT scans acquired at sub-millisievert radiation doses were subjected to DLR, the image quality and lesion detection were superior to images reconstructed with MBIR.

In this study, we evaluated lower dose (LD) hepatic dynamic U-HRCT images reconstructed with DLR, hybrid-IR, and MBIR in comparison with standard-dose (SD) U-HRCT images reconstructed with hybrid-IR as the reference standard to identify the method that allowed for the greatest radiation dose reduction while preserving the diagnostic value.

Materials and methods

We defined 70% of the standard radiation dose (SD) as the LD because in their phantom study, Higaki et al [22] reported that DLR reduced radiation exposure by at least 30% while maintaining the image quality. Our institutional review board approved our observational study in which we applied 70% of the standard radiation dose plus DLR to obtain hepatic dynamic CT scans. Hybrid-IR and MBIR images were reconstructed from the existing raw data. Thus, prior informed patient consent was waived. Patient records and information were anonymized and de-identified prior to analysis.

Study population

All 72 patients had undergone hepatic dynamic U-HRCT studies at our institution. In the SD group (n = 36), the standard radiation dose was used; these patients were seen between April and May 2018. In the LD group (n = 36), we applied 70% of the SD; these patients were seen between July and December 2018.

The patients' age, sex, and body mass index (BMI) were matched between two groups using propensity-score matching. Detailed patient demographics are shown in Table 1.

CT image acquisition

Images were acquired on a U-HRCT scanner (Aquilion Precision, Canon Medical Systems). The acquisition settings have been detailed in a previous paper [16] and are provided in the supplementary material. In summary, we performed hepatic dynamic CT during the hepatic arterial and the equilibrium phase (HAP, EP) in super-high-resolution mode. Tube currents were 250 mA and 175 mA for SDCT and LDCT, respectively. Although pre-enhanced and portal venous phase scans were obtained for the clinical studies, they were not evaluated in ours because they were not performed in super-high-resolution mode.

To assess radiation exposure, we reviewed the CT dose index ($CTDI_{vol}$) and the dose length product (DLP) recorded as Digital Imaging and Communications in Medicine (DICOM) data. We also calculated the size-specific dose estimate (SSDE), an index in which the CTDI is corrected by the body habitus [23, 24]. Size-dependent conversion factors were obtained from AAPM Report 204 [25]; they were based on the sum of the antero-posterior and lateral dimensions at the mid-liver level of each patient.

Image analysis

The standard-dose HAP and EP images were reconstructed with hybrid-IR (Adaptive Iterative Dose Reduction 3-

Table 1 Patient demographics

Clinical features	Lower dose (n = 36)	Standard dose (n = 36)	p value
Age (years)*	70 (43–90)	71 (37–85)	0.61
Gender, male/female	26/10	26/10	1.00
Body mass index (kg/m^2)*	22.2 (18.5–25.7)	22.2 (16.8–27.5)	0.91
Antero-posterior dimension (cm)*	23.7 (20.1–26.7)	23.1 (18.6–26.3)	0.23
Lateral dimension (cm)*	29.4 (25.9–35.4)	29.4 (24.6–33.1)	0.92
Indications for hepatic dynamic CT**			0.54
Follow-up after surgery for malignant liver tumors	19 (52.8)	20 (55.6)	
Evaluation after chemotherapy for malignant tumors	5 (13.9)	6 (16.7)	
Staging of suspected malignant liver tumors	1 (2.8)	0 (0.0)	
Screening for liver tumors	1 (2.8)	3 (8.3)	
Assessment of liver lesions detected on ultrasound studies	10 (27.8)	7 (19.4)	

Unless otherwise indicated, data are number of patients

*Values are the median; the range is shown in parentheses

**Data are number of patients (percent)

Dimensional (AIDR3D, standard setting); Canon Medical Systems); the lower dose HAP and EP images with hybrid-IR, MBIR (forward projected model-based Iterative Reconstruction Solution (FIRST); Canon Medical Systems), and DLR (AiCE).

We compared hybrid-IR, MBIR, and DLR images of the LD group with hybrid-IR images of the SD group as the reference standard. In the SD group, hybrid-IR images were used as the reference standard because they are widely used and represent the standard of care for all CT studies at our institute.

The display monitor was a color LCD monitor featuring the DICOM display mode; the native resolution was 4096 × 2160 pixels; the active display size was 697.9 mm × 368.0 mm (Radiforce RX850, Eizo); the DICOM viewer (RapideyeCore SVIW-DVR01 ver1.5, Canon Medical Systems) was used. The observation conditions were at actual maximum luminance of the LCD monitor (400 cd/m^2); 20–50 lx was the ambient light condition. The conditions for image analysis were the same for all readers.

Qualitative image analysis

Two board-certified radiologists (Y.N. and K.A. with 14 and 31 years of experience in radiology, respectively) and one radiologist (M.A. with 7 years of experience in radiology) performed consensual qualitative analysis of the CT images. They inspected 216 (36 × 2 × 3) images of the LD and 72 (36 × 2 × 1) images of the SD group; the section thickness was 0.25 mm. The readers were blinded to all patient demographics and CT parameters. The images were presented in random order on a preset soft tissue window; the window width and level were 300 and 60 Hounsfield units, respectively.

The readers were given standardized instructions and trained on image sets from 5 patients not included in this study. They ranked the images obtained from the 72 patients for overall image quality on HAP and EP images. The overall image quality was also scored on the 5-point Likert scale [26, 27] where 1 = unacceptable, 2 = subdiagnostic, 3 = average, 4 = above average, and 5 = excellent diagnostic image quality [28].

Quantitative image analysis

Quantitative analysis of transverse images (section thickness 0.25 mm) was performed by one radiologist (K.N. with 6 years of experience in radiology). For attenuation measurements, regions of interest (ROIs) were placed within the aorta, portal vein, liver, and paraspinal muscle. The standard deviation of attenuation measured in the paraspinal muscle represented the image noise. The method for attenuation measurement has been detailed in a previous paper [16] and provided in the supplementary material.

For each image set, the aortic, portal vein (only for EP), and liver contrast-to-noise ratio (CNR) relative to the muscle were calculated using the equation:

$$\mathrm{CNR} = (\mathrm{ROI}_{\mathrm{ORGAN}} - \mathrm{ROI}_{\mathrm{MUSCLE}})/N,$$

where $\mathrm{ROI}_{\mathrm{ORGAN}}$ is the mean attenuation of the organ of interest, $\mathrm{ROI}_{\mathrm{MUSCLE}}$ the mean attenuation of the paraspinal muscle, and N the image noise.

Statistical analysis

We based our study on the hypothesis that the quality of LDCT images reconstructed with DLR would be superior to

the quality of SDCT images reconstructed with hybrid-IR. When superiority was not found, equivalence was assessed with the prespecified margin.

With respect to the image noise, we considered LDCT images to be superior to SDCT images when the entire two-sided 95% confidence interval (CI) for the difference in the image noise between LDCT and SDCT images was below 0; equivalence was recorded when it was within the equivalence range. Similarly, superiority for the CNR and the overall image quality was recorded when the entire two-sided 95% CI of the difference was larger than 0; equivalence was recorded when it was within the equivalence range. At the HAP, the prespecified equivalence margin was set at 3.9, 0.5, 2.5, and 0.5 for the image noise, the CNR of the liver, the aorta, and the overall image quality, respectively. At the EP, the prespecified equivalence margin was set at 3.4, 0.6, 0.6, 0.5, and 0.5 for the image noise, the CNR of the liver, the aorta, the portal vein, and the overall image quality, respectively. These margins were selected as the standard deviation on SDCT images reconstructed with hybrid-IR because we considered a difference smaller than the standard deviation to be clinically negligible.

For qualitative analysis, we calculated the interobserver agreement of our three readers using the weighted kappa statistic to evaluate their agreement. A kappa statistic from 0.81 to 1.00 was interpreted as excellent, from 0.61 to 0.80 as substantial, from 0.41 to 0.60 as moderate, from 0.21 to 0.40 as fair, and from 0.00 to 0.20 as poor agreement [29].

The two-sided Wilcoxon signed rank test was applied to examine the difference in the radiation dose between the LD and the SD groups. Differences of $p < 0.05$ were considered statistically significant. JMP Pro 14 software (SAS Institute) was used for statistical analysis.

Results

Quantitative analysis of the image noise and CNR

Image noise As shown in Table 2, in the HAP and EP, the image noise was lower on LD DLR and LD MBIR images than on the reference SD hybrid-IR images; it was higher on LD hybrid-IR than on the reference images. Consequently, the HAP LD DLR images (95% CI for the difference: − 11.7 to − 8.5) and LD MBIR images (95% CI for the difference: − 5.2 to − 1.5) were superior to reference images while LD hybrid-IR images were neither superior nor equivalent (95% CI for the difference: 2.4–5.7). In the EP, LD DLR images were superior to reference images (95% CI for the difference: − 10.7 to − 8.2), as were LD MBIR images (95% CI for the difference: − 5.2 to − 2.2); LD hybrid-IR images were neither superior nor equivalent to the reference images (95% CI for the difference: 2.8–5.7) (Figs. 1, 2).

Table 2 Image noise, CNR, and overall image quality

	Lower dose			Standard dose
	Hybrid-IR	MBIR	DLR	Hybrid-IR
Image noise (HU)				
HAP	28.9 (24.2–40.3)	21.8 (14.0–34.0)	14.6 (12.3–28.7)	24.8 (18.9–37.9)
EP	28.9 (24.0–37.9)	20.9 (14.9–27.8)	15.1 (12.6–21.1)	25.2 (19.7–33.2)
CNR at HAP				
Aorta	9.4 (6.6–13.9)	13.0 (8.4–21.9)	18.7 (10.0–28.5)	11.9 (5.3–17.9)
Liver	0.8 (-0.3 – 1.3)	0.9 (-0.8 – 1.7)	1.4 (-0.7 – 2.4)	0.8 (-0.2–2.3)
CNR at EP				
Aorta	1.9 (1.0–2.7)	2.4 (1.1–3.9)	3.4 (1.7–4.8)	2.1 (1.0–3.7)
Portal vein	1.9 (1.3–3.0)	2.6 (1.6–4.3)	3.7 (2.3–5.3)	2.2 (1.5–3.6)
Liver	1.1 (− 0.2 – 1.7)	1.5 (− 0.5 – 2.3)	2.0 (− 0.4 – 3.3)	1.2 (− 0.4–2.6)
Overall image quality*				
HAP	3.0 (0.3)	2.4 (0.5)	4.1 (0.5)	3.3 (0.5)
EP	2.9 (0.3)	2.4 (0.5)	4.1 (0.5)	3.4 (0.5)

Unless otherwise indicated, data are the median with ranges in parentheses

HAP hepatic arterial phase, *EP* equilibrium phase

*Data are the mean (standard deviation)

CNR: Liver The CNR of the liver was higher on LD DLR and LD MBIR images than on the reference images (Table 2). LD DLR images acquired in the HAP were superior to the reference images (95% CI for the difference: 0.1–0.7); LD MBIR (95% CI for the difference: − 0.3 to 0.2) and LD hybrid-IR images (95% CI for the difference: − 0.4 to 0.1) were not superior, but equivalent to the reference images. The same was true for EP images (95% CI for the difference: 0.4 to 1.0, − 0.4 to 0.0, and − 0.1 to 0.5 for LD DLR, LD hybrid-IR, and LD MBIR images) (Fig. 3).

CNR: Aorta The aortic CNR was higher on LD DLR and LD MBIR images than on the reference images; on LD hybrid-IR scans, it was lower than on the reference images (Table 2). LD DLR images acquired in the HAP were superior to the reference images (95% CI for the difference: 5.2–8.4), and LD MBIR (95% CI for the difference: − 0.0 to 3.0) and LD hybrid-IR images (95% CI for the difference: − 3.5 to − 1.4) were neither superior nor equivalent to the reference images. In the EP, LD DLR and LD MBIR images were superior to the reference images (95% CI for the difference: 1.0–1.6 and 0.1–0.6, respectively); LD hybrid-IR images were not superior but equivalent to the

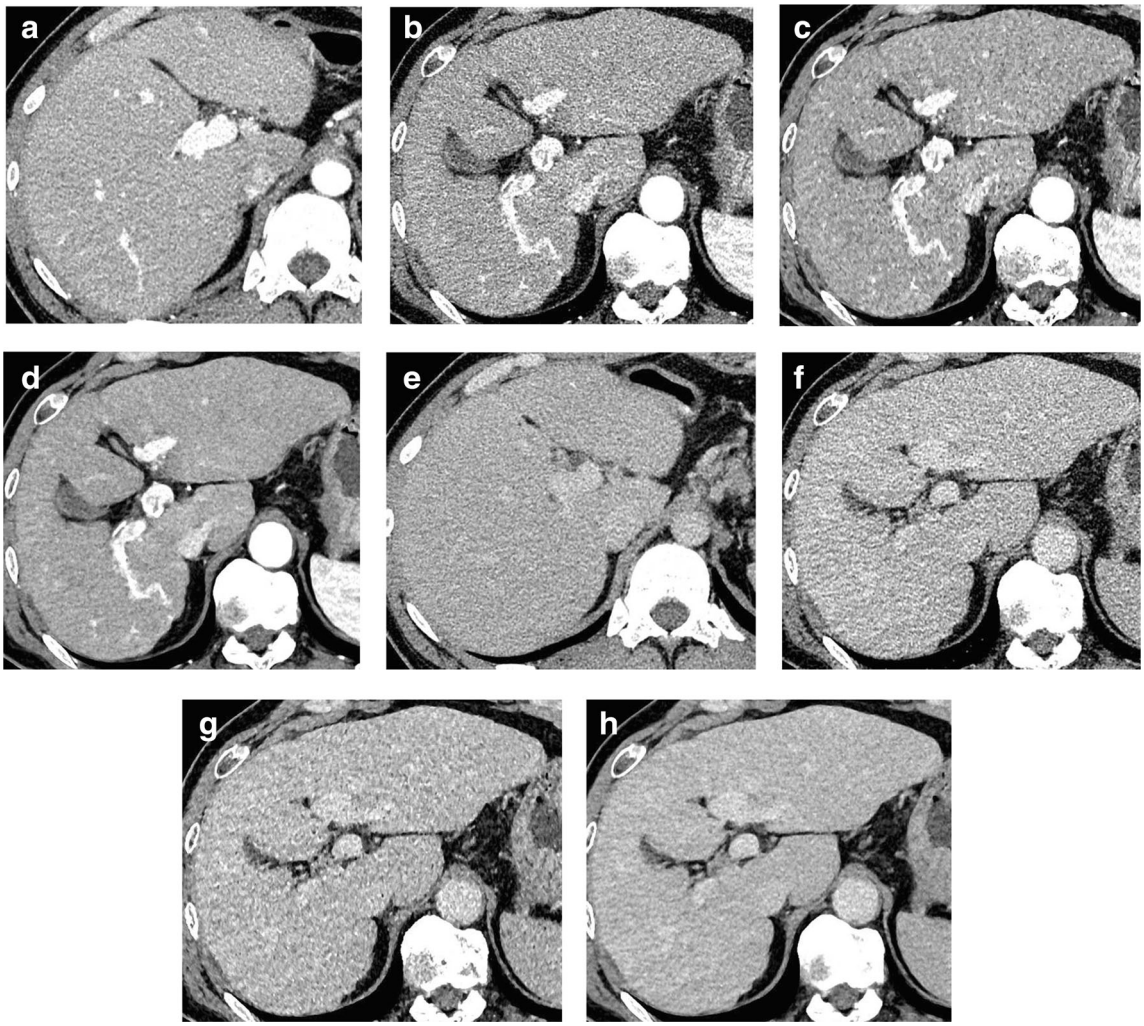

Fig. 1 Hepatic arterial (**a**–**d**) and equilibrium phase images (**e**–**h**) of a 40-year-old man with a BMI of 24.9 (**a**, **e**) and of a 68-year-old man with a BMI of 23.9 (**b**, **c**, **d**, **f**, **g**, and **h**) scanned with the standard radiation dose (SD) (**a**, **e**) or the lower radiation dose (LD) (**b**, **c**, **d**, **f**, **g**, and **h**). Reconstruction was with hybrid-IR (**a**, **b**, **e**, and **f**), MBIR (**c** and **g**), and DLR (**d** and **h**). The image noise was higher on the LD hybrid-IR and MBIR images than on the SD hybrid-IR image; it appeared to be lower on the LD DLR than the SD hybrid-IR image

reference images (95% CI for the difference: − 0.6 to − 0.1) (Fig. 4).

CNR: Portal vein The portal vein CNR at the EP was higher on LD DLR and LD MBIR images and lower on LD hybrid-IR images than on the reference images (Table 2). LD DLR and LD MBIR images were superior to the reference images (95% CI for the difference: 1.1–1.8 and 0.2–0.7, respectively). On the other hand, LD hybrid-IR images were neither superior nor equivalent to the reference image (95% CI for the difference: − 0.5 to − 0.1) (Fig. 5).

Qualitative analysis

The image quality scores at the HAP and EP were higher for LD DLR images and lower for LD MBIR and LD hybrid-IR images than for the reference SD hybrid-IR images (Fig. 1 and Table 2). The scores for LD DLR images acquired in the HAP (95% CI for the difference: 0.5–1.0) and in the EP (95% CI: 0.5–1.0) were superior to the reference images. There was neither superiority nor equivalence in the difference in the image quality scores between LD hybrid-IR and the reference images (95% CI for the difference: − 0.5 to − 0.1) and also between LD MBIR and the reference images (95% CI for the difference: − 1.2 to − 0.7) acquired in the HAP. The same was true for LD hybrid-IR and LD MBIR images acquired in the EP (95% CI for the difference: − 0.7 to − 0.3 and − 1.1 to − 0.7) (Fig. 6).

While all LD DLR images had an average image quality score of 3 or higher both at the HAP and EP, at the HAP, 5.6% of LD hybrid-IR and 58.3% of LD MBIR images were rated as subdiagnostic (score = 2); at the EP, 11.1% of LD hybrid-

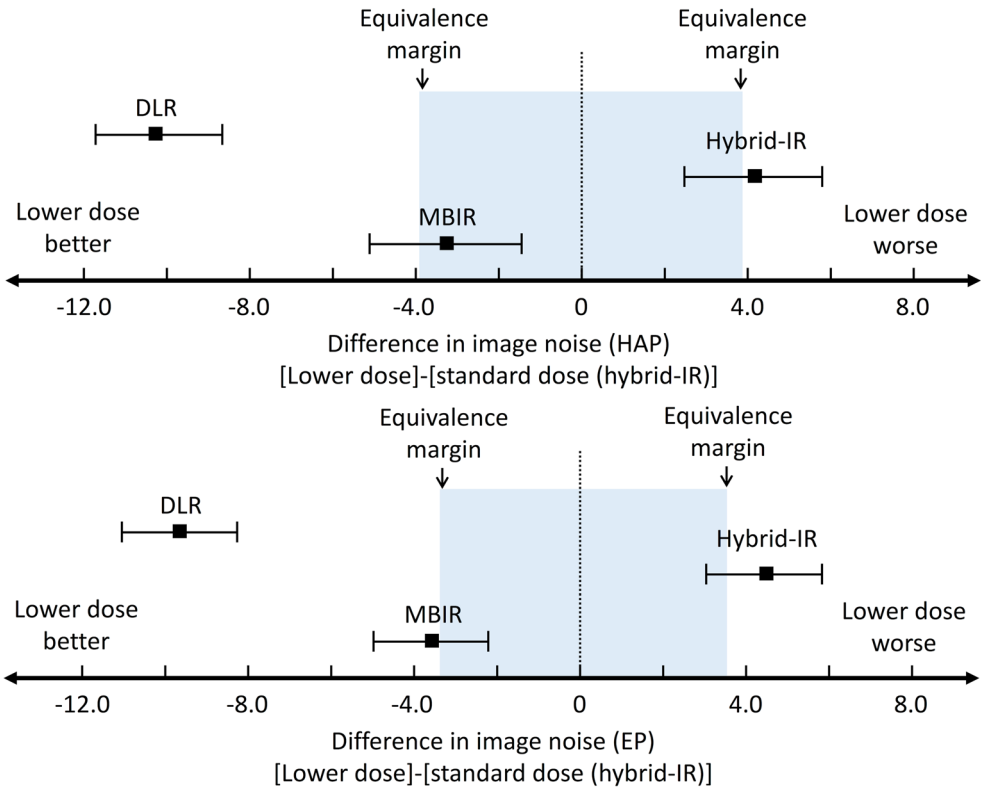

Fig. 2 Superiority and equivalence of the image noise on lower dose (LD) vis-à-vis the reference standard-dose (SD) hybrid-IR images. LD MBIR and LD DLR images were superior to the reference images; LD hybrid-IR images were neither superior nor equivalent to the reference images. HAP hepatic arterial phase, EP equilibrium phase

IR and 55.6% of LD MBIR images were considered subdiagnostic.

Interobserver agreement among the three radiologists was substantial (kappa value range 0.71–0.80).

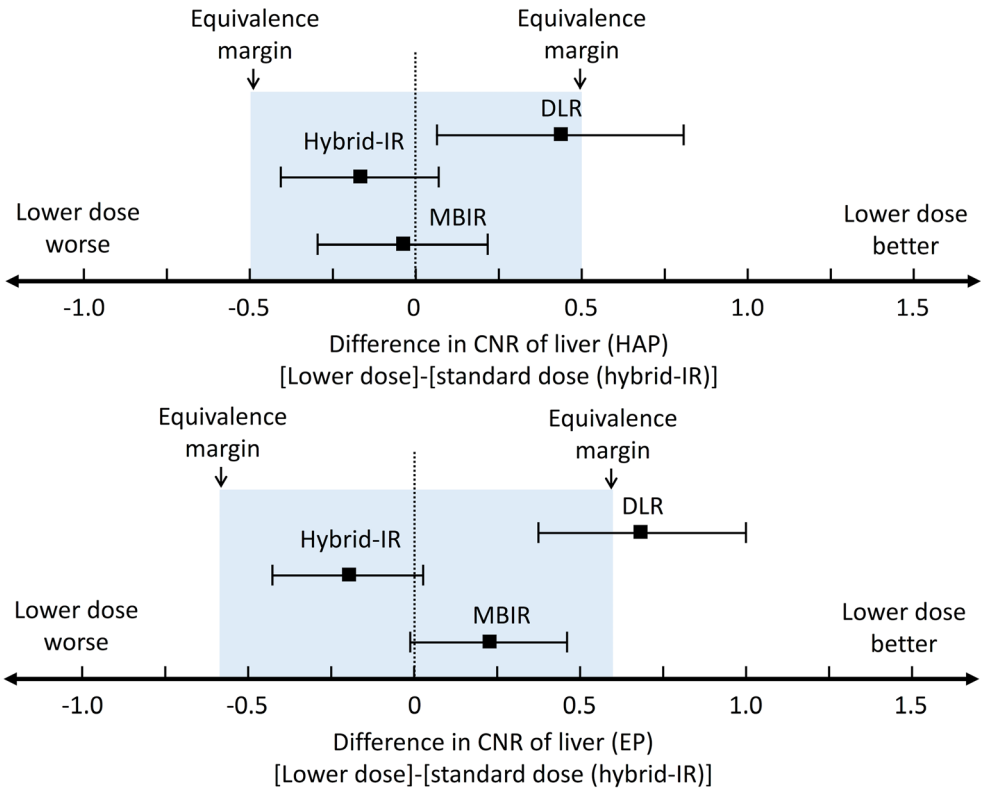

Fig. 3 Superiority and equivalence of the liver contrast-to-noise ratio (CNR) on lower dose (LD) vis-à-vis the reference standard-dose (SD) hybrid-IR images. LD DLR images were superior to the reference images. LD MBIR and LD hybrid-IR images were not superior, but equivalent to the reference images. HAP hepatic arterial phase, EP equilibrium phase

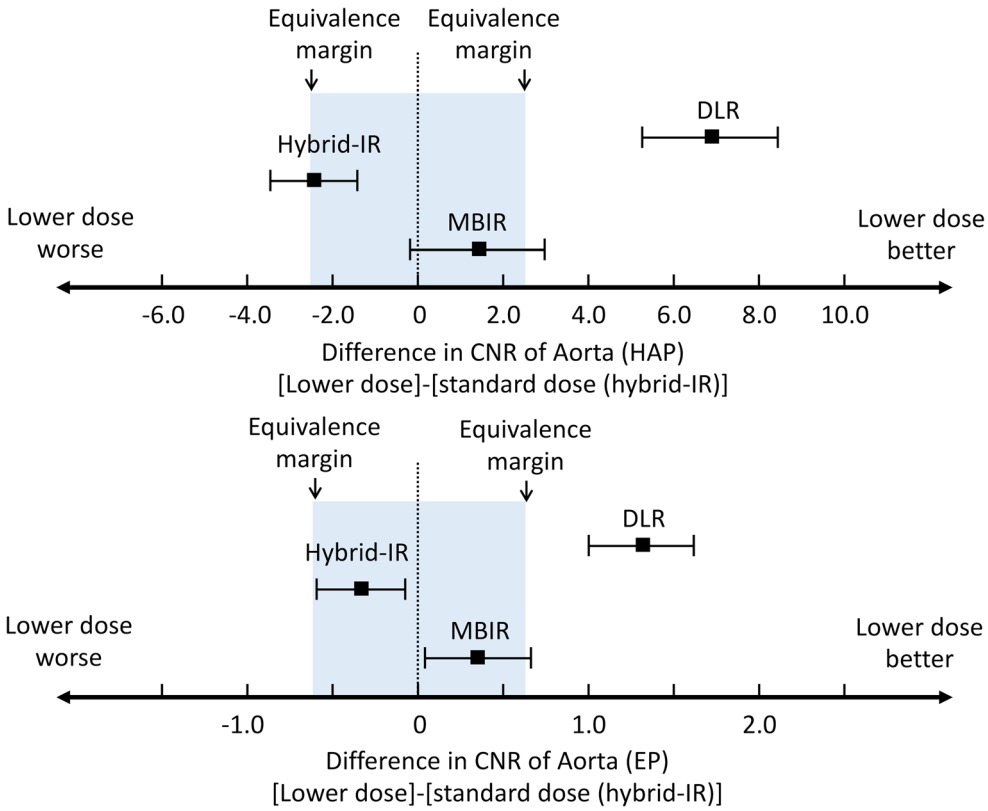

Fig. 4 Superiority and equivalence of the aortic contrast-to-noise ratio (CNR) on lower dose (LD) vis-à-vis the reference standard-dose (SD) hybrid-IR images acquired in the HAP and EP. In the HAP, LD DLR images were superior to the reference images; LD MBIR and LD hybrid-IR images were not. In the EP, LD DLR and LD MBIR images were superior to the reference images and LD hybrid-IR images were not superior, but equivalent. HAP hepatic arterial phase, EP equilibrium phase

Radiation exposure

The median $CTDI_{vol}$, DLP, and SSDE for each phase were 11.3 mGy (range 10.1–15.0), 354.5 mGy cm (range 245.8–513.2), and 17.7 mGy (range 15.3–22.4), respectively, in the LD group; these values were 16.3 mGy (range 13.0–21.7), 495.7 mGy cm (range 378.5–732.5), and 24.6 mGy (range 16.9–30.6) in the SD group, respectively. These values were significantly lower in the LD than the SD group (all $p < 0.01$). Compared to radiation exposure at conventional hepatic dynamic CT studies reported as the Japanese diagnostic reference levels, exposure was lower in the LD and slightly higher in the SD group [30].

Discussion

We found that the image noise was lower and that the CNR and the subjective overall image quality score were higher on LD DLR than the reference SD hybrid IR images. All criteria for superiority were fulfilled on LD-DLR images in both the HAP and EP. Lastly, radiation exposure was lower in the LD group and slightly higher in the SD group than the Japanese diagnostic reference levels [30]. Taken together, DLR appears as an essential reconstruction method for abdominal U-HRCT because DLR can maintain the image quality even with radiation dose reduction.

The image noise was higher and the CNR was lower on LD hybrid-IR than on the reference SD hybrid-IR images and all

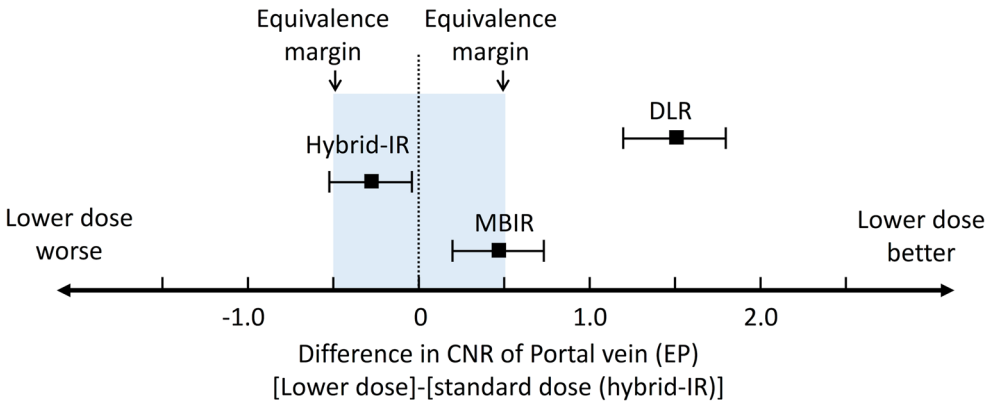

Fig. 5 Superiority and equivalence of the portal-vein contrast-to-noise ratio (CNR) on lower dose (LD) vis-à-vis the reference standard-dose (SD) hybrid-IR images in the EP. LD DLR and LD MBIR images were superior to the reference images. LD hybrid-IR images were neither superior nor equivalent. EP equilibrium phase

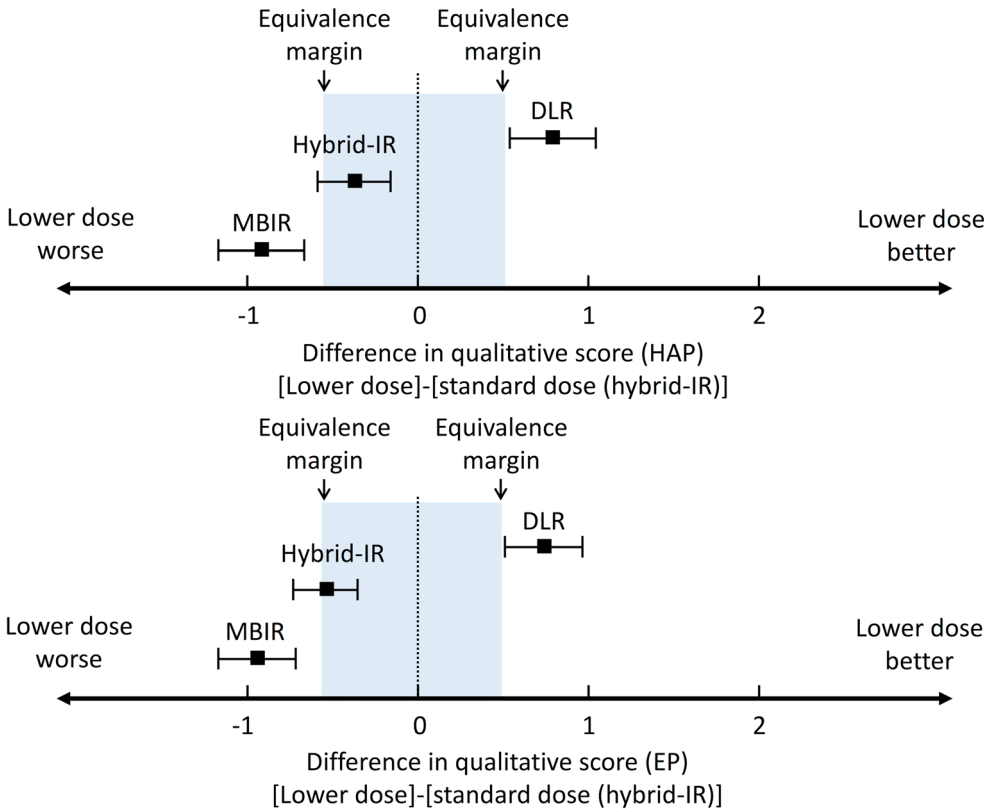

Fig. 6 Superiority and equivalence of the overall image quality score on lower dose (LD) vis-à-vis the reference standard-dose (SD) hybrid-IR images acquired in the HAP and EP. LD DLR images were superior to the reference images. LD MBIR and LD hybrid-IR images were neither superior nor equivalent in both phases. HAP hepatic arterial phase, EP equilibrium phase

criteria for superiority vis-à-vis the reference images were not met. On the other hand, on LD MBIR images, the image noise was lower and the CNR was higher than on the reference images. However, unlike LD DLR images, LD MBIR images were not superior to the reference images with respect to some quantitative parameters; the quality score of LD MBIR images was neither superior nor equivalent to the reference images. Especially at low radiation dose settings, high-frequency noise components, but not low-frequency components, are reduced by MBIR. The latter are effectively suppressed on DLR images [16, 20]. Therefore, we suggest that neither hybrid-IR nor MBIR may allow for radiation dose reduction at abdominal U-HRCT without compromising the image quality.

As the spatial resolution is higher on U-HRCT than conventional CT scans [31, 32], we selected the smallest slice thickness (0.25 mm) to maximize spatial resolution on these scans. We expected the image noise to be much higher on LD U-HRCT than conventional CT scans due to the smaller detector size, the thinner slice thickness, and the lower radiation dose. Indeed, up to 58.3% of hybrid-IR and MBIR images were rated subdiagnostic (overall image quality score = 2). On the other hand, an overall image quality score of 3 (average) or higher was assigned for all LD DLR images. Based on our findings, we suggest that, because it allows for a reduction in the radiation dose and maintains the image quality even at the thinnest slice section, DLR should be applied to abdominal U-HRCT scans.

For the diagnosis of high-contrast lesions at high radiation dose settings, for chest imaging, CT angiography, and for the evaluation of implanted stent grafts, MBIR is superior to other reconstruction methods, including DLR [19, 20]. As Akagi et al [16] and Narita et al [5] reported that the visualization of small arteries and bile ducts on drip-infusion CT cholangiogram images was better subjected to MBIR than DLR, MBIR should be used for the evaluation of small high-contrast lesions on abdominal U-HRCT scans.

We found that with DLR, the radiation dose for abdominal U-HRCT could be reduced to 70% of the standard dose without degradation of the image quality. Epidemiologic studies suggested an association between the incidence of unstable chromosomal aberrations (CAs) in peripheral blood lymphocytes and cancer risks [33, 34]; the radiation dose in routine CT studies significantly increased the number of unstable CAs [35, 36]. Although no direct association between CT-induced adverse biologic changes and cancer risk has been established, the no-threshold hypothesis indicates that radiation exposure must be minimized [37]. Patients with chronic liver disease are monitored with multiple hepatic dynamic CT studies because it is essential for diagnosis as well as evaluation of therapeutic effect of hepatocellular carcinoma [38, 39]. Taken together, radiation dose reduction of abdominal U-HRCT especially for hepatic dynamic scans with DLR even at 30% is supposed to be important clinically.

This observational single-institution study has some limitations. Our study population was relatively small, and we consider our findings to be preliminary. We matched the BMI in the LD and SD groups because not only the radiation dose but also the patient habitus have been reported to affect the image quality [40]. As DLR has been reported to yield similar noise reduction effects irrespective of these factors [18], more studies are needed to determine the effect of DLR based on the patient body size. To avoid excessive complexity, we focused on the effect of image noise reduction on the image quality; we did not evaluate the visibility of specific anatomical structures. According to Akagi et al [16], at the identical radiation dose, the score for vessel conspicuity was the same for DLR and hybrid-IR images, indicating that the visibility of specific anatomical structures may be better on SD hybrid-IR than LD DLR images. Nakamura et al [18] reported that DLR was superior to hybrid-IR for the CT evaluation of hypovascular hepatic metastatic lesions. Due to the absence of pathology findings, we did not assess the usefulness of DLR for the diagnosis of focal hepatic lesions. Further investigation is required focused on the visibility of specific anatomical structures and lesion detectability. As the lower dose protocol using 70% of the standard dose was based on results obtained in a phantom study [22], the accurate dose reduction obtainable at clinical examinations remains to be determined. Although our finding that LD DLR images were superior to SD hybrid-IR images suggests that a further radiation dose reduction may be possible, the potential loss of diagnostic information must be evaluated. Additional studies are needed to determine the radiation dose level at which LD DLR and SD hybrid-IR yield images of similar diagnostic quality.

In conclusion, we demonstrate that the radiation dose for abdominal U-HRCT, especially for hepatic dynamic scans, can be reduced by 30% without degradation of image quality when DLR is applied to the acquired images.

Supplementary Information The online version contains supplementary material available at https://doi.org/10.1007/s00330-020-07566-2.

Funding Dr. Kazuo Awai received a research funding from Canon Medical Systems Co. Ltd.

Compliance with ethical standards

Guarantor The scientific guarantor of this publication is Dr. Kazuo Awai.

Conflict of interest The authors of this manuscript declare relationships with the following companies: Canon Medical Systems Co. Ltd for Kazuo Awai.

The other authors declare that they have no conflict of interest.

Statistics and biometry No complex statistical methods were necessary for this paper.

Informed consent Our institutional review board approved our study in which we applied 70% of the standard radiation dose plus deep learning reconstruction (DLR) to obtain hepatic dynamic CT scans as an observational study. Hybrid iterative reconstruction (hybrid-IR) and model-based IR (MBIR) images were reconstructed from the existing raw data. Thus, prior informed patient consent was waived.

Ethical approval Institutional Review Board approval was obtained.

Methodology
- retrospective
- diagnostic study
- performed at one institution

References

1. Kakinuma R, Moriyama N, Muramatsu Y et al (2015) Ultra-high-resolution computed tomography of the lung: image quality of a prototype scanner. PLoS One 10:e0137165
2. Motoyama S, Ito H, Sarai M et al (2018) Ultra-high-resolution computed tomography angiography for assessment of coronary artery stenosis. Circ J. https://doi.org/10.1253/circj.CJ-17-1281
3. Tanaka R, Yoshioka K, Takagi H, Schuijf JD, Arakita K (2018) Novel developments in non-invasive imaging of peripheral arterial disease with CT: experience with state-of-the-art, ultra-high-resolution CT and subtraction imaging. Clin Radiol. https://doi.org/10.1016/j.crad.2018.03.002
4. Yanagawa M, Hata A, Honda O et al (2018) Subjective and objective comparisons of image quality between ultra-high-resolution CT and conventional area detector CT in phantoms and cadaveric human lungs. Eur Radiol 28:5060–5068
5. Narita K, Nakamura Y, Higaki T, Akagi M, Honda Y, Awai K (2020) Deep learning reconstruction of drip-infusion cholangiography acquired with ultra-high-resolution computed tomography. Abdom Radiol (NY). https://doi.org/10.1007/s00261-020-02508-4
6. Nakayama Y, Awai K, Funama Y et al (2005) Abdominal CT with low tube voltage: preliminary observations about radiation dose, contrast enhancement, image quality, and noise. Radiology 237:945–951
7. Volders D, Bols A, Haspeslagh M, Coenegrachts K (2013) Model-based iterative reconstruction and adaptive statistical iterative reconstruction techniques in abdominal CT: comparison of image quality in the detection of colorectal liver metastases. Radiology 269:469–474
8. Chang W, Lee JM, Lee K et al (2013) Assessment of a model-based, iterative reconstruction algorithm (MBIR) regarding image quality and dose reduction in liver computed tomography. Invest Radiol 48:598–606
9. Fontarensky M, Alfidja A, Perignon R et al (2015) Reduced radiation dose with model-based iterative reconstruction versus standard dose with adaptive statistical iterative reconstruction in abdominal CT for diagnosis of acute renal colic. Radiology 276:156–166
10. Euler A, Stieltjes B, Szucs-Farkas Z et al (2017) Impact of model-based iterative reconstruction on low-contrast lesion detection and image quality in abdominal CT: a 12-reader-based comparative phantom study with filtered back projection at different tube voltages. Eur Radiol 27:5252–5259
11. Mileto A, Guimaraes LS, McCollough CH, Fletcher JG, Yu L (2019) State of the art in abdominal CT: the limits of iterative reconstruction algorithms. Radiology. https://doi.org/10.1148/radiol.2019191422:191422

12. Laurent G, Villani N, Hossu G et al (2019) Full model-based iterative reconstruction (MBIR) in abdominal CT increases objective image quality, but decreases subjective acceptance. Eur Radiol 29: 4016–4025
13. Yasaka K, Furuta T, Kubo T et al (2017) Full and hybrid iterative reconstruction to reduce artifacts in abdominal CT for patients scanned without arm elevation. Acta Radiol 58:1085–1093
14. Nakamoto A, Kim T, Hori M et al (2015) Clinical evaluation of image quality and radiation dose reduction in upper abdominal computed tomography using model-based iterative reconstruction; comparison with filtered back projection and adaptive statistical iterative reconstruction. Eur J Radiol 84:1715–1723
15. Deak Z, Grimm JM, Treitl M et al (2013) Filtered back projection, adaptive statistical iterative reconstruction, and a model-based iterative reconstruction in abdominal CT: an experimental clinical study. Radiology 266:197–206
16. Akagi M, Nakamura Y, Higaki T et al (2019) Deep learning reconstruction improves image quality of abdominal ultra-high-resolution CT. Eur Radiol 29:6163–6171
17. Tatsugami F, Higaki T, Nakamura Y et al (2019) Deep learning-based image restoration algorithm for coronary CT angiography. Eur Radiol 29:5322–5329
18. Nakamura Y, Higaki T, Tatsugami F et al (2019) Deep learning-based CT image reconstruction: initial evaluation targeting hypovascular hepatic metastases. Radiol Artif Intell 1:e180011
19. Nakamura Y, Higaki T, Tatsugami F et al (2020) Possibility of deep learning in medical imaging focusing improvement of computed tomography image quality. J Comput Assist Tomogr 44:161–167
20. Higaki T, Nakamura Y, Zhou J et al (2020) Deep learning reconstruction at CT: phantom study of the image characteristics. Acad Radiol 27:82–87
21. Singh R, Digumarthy SR, Muse VV et al (2020) Image quality and lesion detection on deep learning reconstruction and iterative reconstruction of submillisievert chest and abdominal CT. AJR Am J Roentgenol. https://doi.org/10.2214/AJR.19.21809:1-8
22. Higaki T, Nishimaru E, Nakamura Y et al (2018) Radiation dose reduction in CT using deep learning based reconstruction (DLR): a phantom study. ECR2018. https://doi.org/10.1594/ecr2018/C-1656, https://posterng.netkey.at/esr/viewing/index.php?module=viewing_poster&task=&pi=143052
23. Brady SL, Kaufman RA (2012) Investigation of American Association of Physicists in Medicine Report 204 size-specific dose estimates for pediatric CT implementation. Radiology 265: 832–840
24. Christner JA, Braun NN, Jacobsen MC, Carter RE, Kofler JM, McCollough CH (2012) Size-specific dose estimates for adult patients at CT of the torso. Radiology 265:841–847
25. American Association of Physicists in Medicine (2011) Size-specific dose estimates (SSDE) in Pediatric and adult body CT examinations (Task Group 204). American Association of Physicists in Medicine, College Park, MD https://www.aapm.org/pubs/reports/RPT_204.pdf
26. Phelps AS, Naeger DM, Courtier JL et al (2015) Pairwise comparison versus Likert scale for biomedical image assessment. AJR Am J Roentgenol 204:8–14
27. Likert R (1932) A technique for the measurement of attitudes. Arch Psychol 140:55
28. Hur BY, Lee JM, Joo I et al (2014) Liver computed tomography with low tube voltage and model-based iterative reconstruction algorithm for hepatic vessel evaluation in living liver donor candidates. J Comput Assist Tomogr 38:367–375
29. Svanholm H, Starklint H, Gundersen HJ, Fabricius J, Barlebo H, Olsen S (1989) Reproducibility of histomorphologic diagnoses with special reference to the kappa statistic. APMIS 97:689–698
30. Japan Association on Radiological Protection in Medicine (2015) Diagnostic reference levels based on latest surveys in Japan: Japan DRLs 2015. http://www.radher.jp/J-RIME/report/DRLhoukokusyoEng.pdf
31. Yoshioka K, Tanaka R, Takagi H et al (2018) Ultra-high-resolution CT angiography of the artery of Adamkiewicz: a feasibility study. Neuroradiology 60:109–115
32. Tamm EP, Rong XJ, Cody DD, Ernst RD, Fitzgerald NE, Kundra V (2011) Quality initiatives: CT radiation dose reduction: how to implement change without sacrificing diagnostic quality. Radiographics 31:1823–1832
33. Bonassi S, Norppa H, Ceppi M et al (2008) Chromosomal aberration frequency in lymphocytes predicts the risk of cancer: results from a pooled cohort study of 22 358 subjects in 11 countries. Carcinogenesis 29:1178–1183
34. Fucic A, Bonassi S, Gundy S et al (2016) Frequency of acentric fragments are associated with cancer risk in subjects exposed to ionizing radiation. Anticancer Res 36:2451–2457
35. Abe Y, Noji H, Miura T et al (2019) Investigation of the cumulative number of chromosome aberrations induced by three consecutive CT examinations in eight patients. J Radiat Res 60:729–739
36. Sakane H, Ishida M, Shi L et al (2020) Biological effects of low-dose chest CT on chromosomal DNA. Radiology 295:439–445
37. Valentin J (2005) Low-dose extrapolation of radiation-related cancer risk. Ann ICRP 35:1–140
38. Marrero JA, Kulik LM, Sirlin CB et al (2018) Diagnosis, staging, and management of hepatocellular carcinoma: 2018 Practice Guidance by the American Association for the Study of Liver Diseases. Hepatology 68:723–750
39. Heimbach JK, Kulik LM, Finn RS et al (2018) AASLD guidelines for the treatment of hepatocellular carcinoma. Hepatology 67:358–380
40. Qurashi AA, Rainford LA, Alshamrani KM, Foley SJ (2018) The impact of obesity on abdominal CT radiation dose and image quality. Radiat Prot Dosimetry. https://doi.org/10.1093/rpd/ncy212